Brownian Dynamics Simulations of Interaction Between Scorpion Toxin Lq2 and Potassium Ion Channel

Meng Cui,* Jianhua Shen,* James M. Briggs,† Xiaomin Luo,* Xiaojian Tan,* Hualiang Jiang,* Kaixian Chen,* and Ruyun Ji*

*Center for Drug Discovery and Design, State Key Laboratory of New Drug Research, Shanghai Institute of Meteria Medica, Shanghai Institutes for Biological Sciences, Chinese Academy of Sciences, Shanghai 200031, Peoples Republic of China; and †Department of Biology and Biochemistry, University of Houston, Houston, Texas 77204-5513 USA

ABSTRACT The association of the scorpion toxin Lq2 and a potassium ion (K^+) channel has been studied using the Brownian dynamics (BD) simulation method. All of the 22 available structures of Lq2 in the Brookhaven Protein Data Bank (PDB) determined by NMR were considered during the simulation, which indicated that the conformation of Lq2 affects the binding between the two proteins significantly. Among the 22 structures of Lq2, only 4 structures dock in the binding site of the K^+ channel with a high probability and favorable electrostatic interactions. From the 4 candidates of the Lq2-K^+ channel binding models, we identified a good three-dimensional model of Lq2-K^+ channel complex through triplet contact analysis, electrostatic interaction energy estimation by BD simulation and structural refinement by molecular mechanics. Lq2 locates around the extracellular mouth of the K^+ channel and contacts the K^+ channel using its β-sheet rather than its α-helix. Lys27, a conserved amino acid in the scorpion toxins, plugs the pore of the K^+ channel and forms three hydrogen bonds with the conserved residues Tyr78(A–C) and two hydrophobic contacts with Gly79 of the K^+ channel. In addition, eight hydrogen-bonds are formed between residues Arg25, Cys28, Lys31, Arg34 and Tyr36 of Lq2 and residues Pro55, Tyr78, Gly79, Asp80, and Tyr82 of K^+ channel. Many of them are formed by side chains of residues of Lq2 and backbone atoms of the K^+ channel. Thirteen hydrophobic contacts exist between residues Met29, Asn30, Lys31 and Tyr36 of Lq2 and residues Pro55, Ala58, Gly79, Asp80 and Tyr82 of the K^+ channel. These favorable interactions stabilize the association between the two proteins. These observations are in good agreement with the experimental results and can explain the binding phenomena between scorpion toxins and K^+ channels at the level of molecular structure. The consistency between the BD simulation and the experimental data indicates that our three-dimensional model of Lq2-K^+ channel complex is reasonable and can be used in further biological studies such as rational design of blocking agents of K^+ channels and mutagenesis in both toxins and K^+ channels.

INTRODUCTION

Compared with other ion channel families, potassium ion (K^+) channels represent a very large and diverse collection of membrane proteins whose basic biological task is to allow K^+ to flow selectively across the cell membrane. K^+ channels are involved in a large number of important cellular functions, such as control of cell electrical excitability, excitation/response coupling, and electrical signaling. The permeability of K^+ crossing the K^+ channels is thus associated with many essential biological processes, such as regulation of neuronal and cardiac electrical patterns, the release of some neurotransmitters, muscle contractility, hormone and fluid secretion and, in non-electrically excitable cells, modulation of signal transduction pathways (Kaczorowski and Garcia, 1999). Because of the pivotal role that potassium channels play in biological systems, these channels have long been attractive targets for the rational design of new drugs based on their structures and interaction mechanisms. Our interest in the mechanism of blockage of K^+ channels stems from our efforts to design new ion channel blockers that selectively interact with K^+ channels, with the eventual aim of developing new drugs for treatment of cardiovascular diseases. In particular, our research is focused on the application of molecular simulation and modeling methods in the rational design of new blocking agents of K^+ channels.

Some naturally occurring peptide toxins can inhibit ion channels. Over the past decade, numerous peptide inhibitors of Ca^{2+}, Na^+, and K^+ channels have been discovered. These toxins are highly specific for their targeting ion channels, and they are effective at nanomolar concentrations. Accordingly, these peptide inhibitors have been widely used for pharmacologically distinguishing the different channels in a cell's membrane (Mintz et al., 1992) and for mapping the membrane folding topology combined with the ion channel mutagenesis (Catterall, 1988; MacKinnon and Miller, 1989; MacKinnon et al., 1990).

Lq2 is a unique scorpion toxin, one member of the Charybdotoxin (CTX) family of scorpion toxins. Acting on the extracellular side, Lq2 blocks the ion conduction pore not only in the voltage- and Ca^+-activated K^+ channels, but also in the inward-rectifier K^+ channels. Because of its property of binding all three kinds of K^+ channels, Lq2 can be used as a structural probe to examine how the nonconserved pore-forming sequences are arranged in space to

Received for publication 5 July 2000 and in final form 4 January 2001.

Address reprint requests to Prof. Hualiang Jiang, Shanghai Institute of Meteria Medica, Chinese Academy of Sciences, 294 Taiyuan Road, Shanghai 200031, P. R. China. Tel.: +86-21-64311833-222; Fax: +86-21-64370269; E-mail: jiang@iris3.simm.ac.cn or hljiang@mail.shcnc.ac.cn.

0006-3495/01/04/1659/11 $2.00

form similar pore structures. Therefore, an understanding of the molecular interactions between Lq2 and K^+ channels will provide insights not only into the conservation of the architecture of K^+ pores, but also into the mechanisms underlying the specificity of channel-toxin interaction. The solution structure of Lq2 has recently been determined by nuclear magnetic resonance (NMR) techniques (PDB code: 1LIR), and it will now be especially informative to identify the residues involved in the toxin's channel blocking function (Renisio et al., 1999).

However, no experimental data for the structure of Lq2-K^+ channel complexes have been reported. In this study, by means of the Brownian dynamics (BD) method (Ermak and McCammon, 1978), we have simulated the association of Lq2 (all of the 22 available structures in the PDB; 1LIR) and KcsA, the structure of which was modified according to the experiment of MacKinnon et al.(1998), for the aim of obtaining three-dimensional (3D) models of Lq2-K^+ channel complexes as the first step in designing new blockers of K^+ channels. We used the docking feature of BD simulation (Pearson and Gross, 1998; Ouporov et al., 1999) and the structural refinement functionality of molecular mechanics to identify the amino acid residues involved in complex formation, localize the regions of binding, and estimate the strength of binding between the scorpion toxin Lq2 and the K^+ channel.

MATERIALS AND METHODS

Atomic coordinates

The atomic coordinates of the scorpion toxin Lq2 (Renisio et al., 1999) and the K^+ channel KcsA (Doyle et al., 1998) were obtained from the Protein Data Bank at the Brookhaven National Laboratory (Bernstein et al., 1977), entries 1LIR and 1BL8, respectively.

Lq2 consists of an α-helix (residues Ser10 to Leu20) and a β-sheet, connected by an $\alpha\beta$3 loop (residues Asn22 to Asn24). The β-sheet has two well-defined anti-parallel strands (residues Gly26 to Met29 and residues Lys32 to Cys35), which are connected by a type I′ β-turn centered between residues Asn30 and Lys31. The N-terminal segment (residues Pca1 to Thr8) appears to form a quasi-third strand of the β-sheet (Renisio et al., 1999). Entry 1LIR contains 22 conformations of scorpion toxin Lq2, which were obtained from the nuclear magnetic resonance (NMR) spectroscopy; all of these structures were used in the BD simulations.

Among the K^+ channels, the three-dimensional (3D) structure of the KcsA K^+ channel, a protein isolated from the bacterium *Streptomyces lividans*, was the first determined by x-ray crystallography at 3.2 Å resolution (Doyle et al., 1998). The KcsA channel is a tetramer containing four identical subunits arranged symmetrically around the central pore. Each subunit consists of two transmembrane α-helices (TM1 and TM2), linked by a short stretch of ~30 amino acids that form a helical pore and an extracellular loop (known as the turret). The four TM2 helices are arranged in such a way that they form the poles of an inverted teepee. This crystal structure provides a solid framework for the models of the K^+-selective channels and, for the first time, gives indisputable evidence that the ion permeation pathway across the membrane is indeed at the center of four identical subunits that cluster around the narrowest part of the pore formed by the pore (P) loop. Mutagenesis studies suggest that the "ion-selective filter" is located at the external end of the pore and formed by the conserved signature sequence, T-X-X-T-X-G-Y/F-G, within the pore region (Heginbotham et al., 1992, 1994). KcsA shares signature sequences with eukaryotic K^+ channels that are responsible for ion selectivity and pore formation. Despite the lack of conservation of the sequence in the P-region, the structure of the outer pore of K^+ channels appears to be conserved. This conclusion was based on the observation that a scorpion toxin, Lq2, can bind to the external part of the K^+ pore in all three of the channel types: voltage-activated, Ca^{2+}-activated, and inward-rectifier K^+ channels (Lucchesi et al., 1989; Escobar et al., 1993; Lu and MacKinnon, 1997). Further evidence is that experiments conducted by MacKinnon et al. (1998) showed that the KcsA K^+ channel pore structure and extracellular entryway were very similar to that of eukaryotic voltage-gated K^+ channels, such as the *Shaker* K^+ channel from *Drosophila* and vertebrate voltage-gated K^+ channels. In addition, through MALDI-TOF mass spectrometry determination, MacKinnon et al. (1998) also found that the triple mutated form of KcsA can be complexed with Lq2. We can, therefore, build a 3D model for the eukaryotic K^+ channels according to the x-ray crystal structure of KcsA (Doyle et al., 1998) and the mutagenesis results of Mackinnon et al. (1998) for the sake of studying the interactions between Lq2 and a K^+ channel.

Residues Arg27, Ile60, Arg64, Glu71, and Arg117, missing in the current KcsA x-ray structure, were added using the Biopolymer module of SYBYL Release 6.5 (Tripos Inc., St. Louis, MO). The 3D structural model of eukaryotic K^+ channels was generated, viz., mutations of Gln58Ala (Q58A), Thr61Ser (T61S), and Arg64Asp (R64D) with the Biopolymer module of SYBYL based on the x-ray structure of the KcsA K^+ channel and the mutagenesis experiments of Mackinnon et al. (1998). The modified residues of the K^+ channel were subjected to energy refinement (the gradient tolerance was set to 0.05 kcal/(mol*Å)) using the adopted-basis Newton Raphson algorithm and the CHARMm22 force field in Quanta (1998 Release; Molecular Simulation, Inc., San Diego, CA) to relieve possible steric clashes and overlaps.

BD simulation

The program package MacroDox version 3.2.2 (Northrup et al., 1999) was used to assign the titratable charges on proteins, solve the linearized Poisson-Boltzmann equation, and run the various Brownian dynamics simulations for the association between the scorpion toxin Lq2 and a K^+ channel. The BD algorithm for this program has been detailed by Northrup et al. (1987, 1993). The new updated charge file of CHARMm22, which includes the charges of nonstandard residues such as PCA, was used to assign the charges of the K^+ channel and Lq2. The surface-accessibility-modified Tanford-Kirkwood (TK) calculations were performed using the method of Matthew (Matthew, 1985; Matthew and Gurd, 1986) to determine the protonation status of each titratable residue in the two proteins at pH 7.0 and ionic strength 0.1 M. Lq2 has three disulfide bonds, so the charges of the sulfur atoms of residues Cys7, Cys13, Cys17, Cys28, Cys33, and Cys35 were zeroed out. The TK recommended partial charges were assigned to the K^+ channel and formal charges were assigned to Lq2. The total charge is $-3.6e$ for the K^+ channel, and 5.0e for each of the 22 structures of Lq2.

After charge assignments, the electrostatic potentials about the K^+ channel and Lq2 were determined by numerically solving the linearized Poisson-Boltzmann equation,

$$-\nabla \cdot \varepsilon \nabla \phi + \varepsilon \kappa^2 \phi = \rho \qquad (1)$$

where ϵ is the dielectric constant, κ is the inverse Debye length, ϕ is the electrostatic potential, and ρ is the charge density. Taking the above assigned charges as initial values, Eq. 1 was solved by the method of Warwicker and Watson (1982) as implemented in the MacroDox program (Northrup et al., 1999). The electrostatic potentials were determined on $61\times61\times61$ cubic grids centered on the center of mass of the two proteins. The protein interior dielectric constant and solvent dielectric constants were 4.0 and 78.3, respectively. The resolutions of inner grid and outer grid

for the K^+ channel were chosen as the default values in the MacroDox program, 1.3 and 3.9 Å, respectively. Electrostatic focusing was used such that a low resolution grid (3.9 Å spacing between grid points) was generated first and then used to obtain more accurate boundary potentials for a second, higher resolution focused grid (1.3 Å spacing). The UHBD program (Madura et al., 1995) was used to calculate the electrostatic potentials for the proteins according to the assigned charges. The electrostatic potentials determined by UHBD, as shown in Fig. 1, were visualized by GRASP program (Nicholls et al., 1991).

The BD simulation of the two interacting macromolecules in a solvent was run stochastically by a series of small displacements chosen from a distribution that is equivalent to the short time solution of the Smoluchowski diffusion equation (Smoluchowski, 1917) derived from different forces. The basic Ermak-McCammon algorithm (Ermak and McCammon, 1978) was employed to simulate the translational Brownian motion of two interacting proteins as the displacements Δr of the relative separation vector $\mathbf{r}$ between the centroids of the two proteins in a time step Δt according to the relation

$$\Delta \mathbf{r} = \frac{D \cdot \Delta t}{k_B T} \cdot \mathbf{F} + \mathbf{S} \tag{2}$$

where D is the translational diffusion coefficient for the relative motion and assumed to be spatially isotropic, $\mathbf{F}$ is the systematic inter-particle force, which is computed from the electrostatic field calculated before Brownian dynamics, $k_B T$ is the Boltzmann constant times absolute temperature, and $\mathbf{S}$ is the stochastic component of the displacement arising from collisions of proteins with solvent molecules, which is generated by taking normally distributed random numbers obeying the relationship.

$$\langle \mathbf{S}^2 \rangle = 2D\Delta t \tag{3}$$

$$\langle \mathbf{S} \rangle = 0$$

A similar equation governs the independent rotational Brownian motion of each particle, in which the force is replaced by a torque and D is replaced by an isotropic rotational diffusion coefficient D_{ir} for each particle i.

Next, BD simulations of Lq2 binding to the K^+ channel were performed to identify the favorable complex(es). For simulations of protein-protein interactions, the two proteins were treated as rigid bodies. Therefore, the translational and rotational motions can be simulated for one of the proteins (protein II) around the other (protein I) (Gabdoulline and Wade, 1998; Fig. 2). In this study we defined the larger protein, K^+ channel as protein I (i.e., the fixed protein) and the smaller protein, Lq2, as protein II (i.e., the diffusing protein).

Trajectories were started with Lq2 at a random position and orientation on the b-surface (Fig. 2), a sphere of radius b (71 Å) centered on the K^+ channel at which the forces due to the K^+ channel are centrosymmetric. The mobile Lq2 was subject to three forces: the electrostatic attraction between the two proteins, the random Brownian force, and the frictional force due to solvent viscosity. The closest approach of the mobile protein Lq2 to the fixed receptor K^+ channel was recorded, and the trajectory was terminated when the mobile ligand escaped the q-sphere (200 Å). The Bdtirm 8.2 module (BD of 2 irregular rotating macromolecules) of the MacroDox program was used to simulate the interactions between scorpion toxin Lq2 and the K^+ channel at pH 7.0 and 0.1 M ionic strength. All 22 structures of Lq2 in 1LIR were docked with the K^+ channel, respectively, typically by running 3000 trajectories. In addition to visual examination of the structures of the final complexes, statistical analyses were performed using the review module of MacroDox. The statistical analyses resulted in the number of occurrences that each amino acid residue formed intermolecular contacts between proteins in the complexes.

Structure refinement for the final complex

To explore the mechanism of interaction of Lq2 and the K^+ channel in more detail, the final structure of the complex, obtained from BD simulations, was subjected to energy refinement using the adopted-basis Newton Raphson algorithm and CHARMm22 force field in Quanta. During the structure refinement, a distance-dependent dielectric constant of 4 was used to simulate the solvation effect, and the gradient tolerance was set to 0.05 kcal/(mol·*Å). The details of the interaction were analyzed using the LIGPLOT program (Wallace et al., 1995; McDonald and Thornton, 1994).

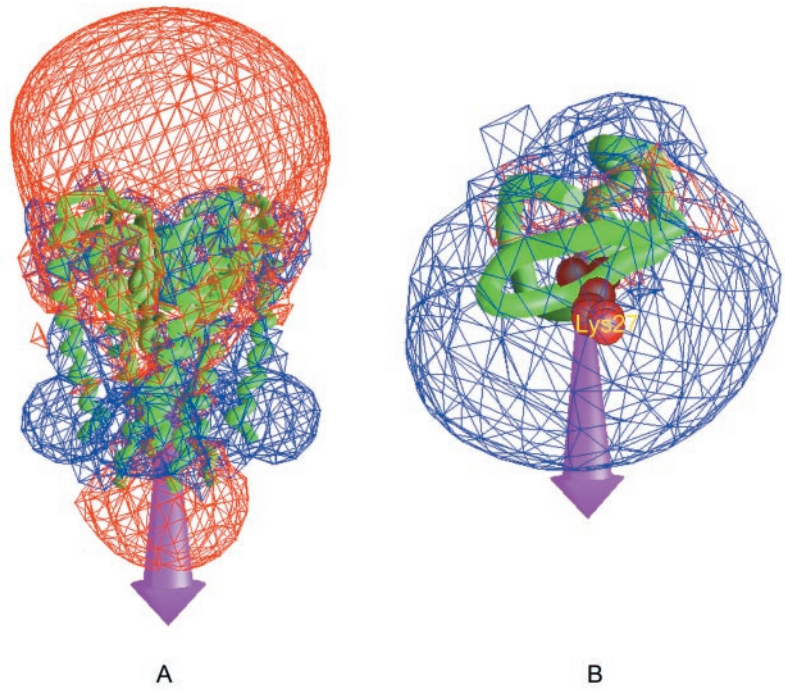

FIGURE 1 The electrostatic potential contour maps for the K^+ channel and the scorpion toxin Lq2. (*A*) Electrostatic potential for the K^+ channel. The red contours represent isopotential surfaces where charge 1e possesses electrostatic free energy equal to −1.0 kT/e; the blue isopotential surfaces are for energy +1.0 *kT*/*e*. (*B*) Electrostatic potential for the scorpion toxin Lq2. The red contours represent isopotential surfaces where charge 1e possesses electrostatic free energy equal to −2.0 kT/e; the blue isopotential surfaces are for energy +2.0 kT/e. Arrows indicate the directions of the dipoles in the proteins. The figure was generated with the program GRASP (Nicholls et al., 1991).

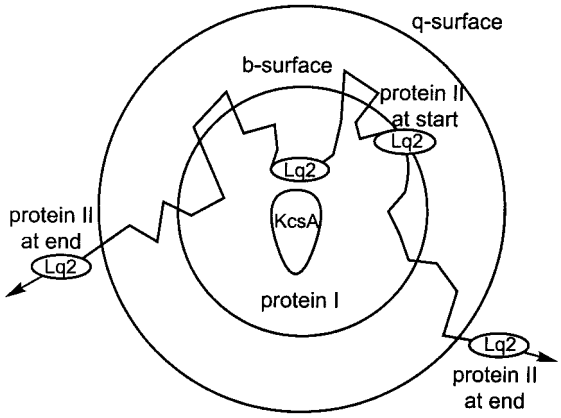

FIGURE 2 A systematic representation of the Brownian dynamics simulation of the association between scorpion toxin Lq2 and the K^+ channel. Simulations are conducted in coordinates defined relative to the position of the center of the protein, the K^+ channel (protein I). At the beginning, each trajectory of the second mobile protein (protein II), Lq2, is positioned with a randomly chosen orientation at a randomly chosen point on the surface of the inner sphere of radius *b* (71 Å in this work). BD simulation is then performed until this protein diffuses outside the outer sphere of radius *q* (200 Å in this work). During the simulation, satisfaction of reaction criteria for encounter complex formation is monitored. The complex(es) with the smallest reaction distance are recorded.

RESULTS AND DISCUSSION

Electrostatic potentials

During the BD simulations, the proteins are treated as rigid bodies, so the effect of their flexibility is not considered. To overcome this shortcoming, we considered all of the 22 available NMR conformations of the Lq2 scorpion toxin in solution when performing the BD simulations. For the K^+ channel, because it is embedded in the membrane of the cell, it should not be substantially flexible.

The appearance of the electrostatic potential on the surface of the K^+ channel protein and the scorpion toxin Lq2 are given in Fig. 1. As expected, the mouth of the K^+ channel, which is outside the cell membrane, bears a large negative electrostatic potential, whereas the surface of Lq2, on the contrary, has a large positive electrostatic potential. The negative electrostatic potential is centrosymmetric around the central axes of the K^+ channel (Fig. 1 *A*). In addition, the electrostatic potential inside the channel is negative, and that outside the channel is positive. This attracts the positively charged potassium ion to the channel opening and is beneficial for the channel to interact with the negatively charged head groups of the lipid bilayer in the cell membrane. For Lq2, the positive electrostatic potential results mainly from the side chains of residues Arg25, Lys27, Lys31, and Arg34, and is centered around the side chain of Lys27 (Fig. 1 *B*). This indicates that Lq2 may associate with the entryway of the K^+ channel using the positive patch around the side chain of Lys27. This conclusion was validated by the BD simulations (see discussion below). Moreover, the electrostatic potentials of both Lq2 and the K^+ channel indicate that the electrostatic attraction force may be important for the association of Lq2 to the K^+ channel from the viewpoint of Coulombic interactions.

BD-identified Lq2-K^+ channel complexes

The center of mass of Lq2 and the position of the oxygen atom of the water in the selection filter of the x-ray crystallographic structure of KcsA were chosen as the monitors of association during the BD simulations. In order to avoid unfavorable complexes formed by Lq2 with the intracellular surface of the K^+ channel, the separation defining a complex was set to 30 Å. This distance is large enough to get the most significant complexes from the simulations, as shown later.

During the initial BD runs, we found that the electrostatic attraction is so large that the simulations ran endlessly at pH 7.0, 0.1 M, and 298.15 K. When the binding patches of the two proteins are close to each other, the stochastic force is not large enough to overcome the electrostatic force, so Lq2 could not escape the binding site of the K^+ channel. Either of two methods can be used to solve this problem: (i) simulate this system at sufficiently high salt concentration (the salt dampens the field), so the interaction can be limited by the association rate rather than dissociation; or (ii) increase the simulation temperature so as to make the stochastic force large enough to overcome the electrostatic force. The first approach is typically used when studying the reactive rate of the association of two proteins. The main purpose of this study was to obtain the complexes in order to aid in understanding the mechanism of the interaction between the two proteins. Therefore, we used the second approach, increasing the simulation temperature to 500 K throughout all of the simulations.

BD simulations were performed for each conformation of Lq2 derived from NMR studies (1LIR). The most favorable triplet of contacts in all Lq2 complexes with the K^+ channel are listed in Table 1. Among the 22 conformations of Lq2, the 5th, 7th, 15th, and 16th structures have a high frequency (probability) of satisfying the criterion of association, an interaction distance between the two proteins of less than 30 Å (Table 1). The average electrostatic interaction free energies between these four structures of Lq2 and the K^+ channel are all less than -22 kcal/mol (Table 1 and Fig. 3). The distribution of Lq2 (e.g., the 16th structure) around the K^+ channel is shown in Fig. 4, from which we can see that the largest distribution is the one in which the proteins are closer than 20 Å. This supports the selected interaction criterion, <30 Å.

In order to get a favorable Lq2-K^+ channel complex, we performed a detailed triplet contact analysis for each of above four structures of Lq2 interacting with the K^+ channel, because three close interactions define the relative geometry of the Lq2-K^+ channel complex, whereas one or

TABLE 1 Possible triplet contacts between each structure of Lq2 and modified KcsA K^+ channel at 0.1 M ionic strength

Structures	Triplets (K^+ channel res-Lq2 res)			F	G_{elec}
1	D80-R25	G79-R34	P55-K31	41	−15.7
	D80-R34	G79-K27	A57-R25	39	−15.1
	D80-R34	P55-S37	A57-R25	36	−15.0
	G79-R34	G56-K32	A57-R25	33	−15.7
2	G79-K27	D80-3K1	P55-K32	50	−20.8
	G79-K18	Y78-R19	D80-E5	28	−16.2
3	G79-K27	D80-R34	P55-S37	102	−20.2
	G79-R34	Y78-K27	P55-S37	61	−20.9
	G79-K27	D80-R34	A57-R25	58	−20.7
	G79-R34	Y78-K27	A57-R25	43	−21.0
4	G79-R19	Y78-K18	P55-R25	50	−20.5
	G79-K18	Y78-R19	D80-E5	38	−17.2
	G79-K27	D80-R25	P55-S37	27	−14.3
5	G79-K27	D80-P25	G56-K31	72	−22.8
	G79-K27	D80-R34	P55-K31	34	−20.8
	G79-K27	D80-P25	Y78-R34	32	−21.4
6	G79-K27	P55-K31	D80-R34	110	−19.5
	Y78-K27	P55-K31	D80-R34	73	−20.0
	G79-K27	P55-S37	D80-R34	38	−19.3
7	G79-K27	D80-R34	A57-R25	57	−22.0
	G79-K27	P55-S37	A57-R25	44	−22.3
	G79-K27	D80-R34	P55-S37	37	−22.2
	G79-R34	Y78-K27	G56-R25	37	−22.2
	D80-R34	P55-S37	A57-R25	31	−22.2
8	G79-K18	Y78-R19	P55-K31	63	−22.0
	G79-K18	Y78-R19	D80-E5	26	−20.8
9	G79-R19	D80-E5	A54-K31	50	−15.4
	G79-K27	D80-R34	P55-S37	23	−12.9
10	G79-K18	D80-E5	Y78-R19	40	−17.0
	G79-R19	Y78-K18	P55-R25	21	−17.9
11	G79-K27	D80-R34	P55-S37	36	−16.3
	G79-K27	D80-R34	P55-R25	23	−15.6
12	G79-K27	D80-R34	A57-R25	101	−18.8
	G79-K27	D80-R34	G56-K32	50	−18.8
	G79-K27	P55-K32	A57-R25	48	−18.9
	G79-K27	G56-K32	A57-R25	44	−18.9
	D80-R34	G56-K32	A57-R25	43	−18.9
13	G79-K27	P55-K31	D80-R34	39	−17.7
	G79-K27	P55-S37	A57-R25	26	−16.8
	G79-K27	P55-S37	D80-R25	25	−17.0
14	G79-K27	D80-R34	P55-S37	47	−16.4
	G79-K27	D80-R34	A57-R25	11	−14.6
15	Y78-K27	D80-R34	P55-K31	232	−23.6
	G79-K27	D80-R34	P55-K31	28	−23.4
16	G79-K27	P55-25	D80-R34	126	−22.5
	G79-R34	Y78-27	P55-R25	91	−23.2
17	G79-R34	80-K32	P55-S37	15	−16.2
	G79-K27	80-R34	P55-K32	12	−16.0
18	G79-K27	P55-S37	D80-R34	149	−20.4
	G79-K27	P55-S37	A57-R25	108	−20.4
	G79-K27	D80-R34	A57-R25	90	−20.4
	P55-S37	D80-R34	A57-R25	90	−20.4
19	G79-K27	D80-R34	A57-R25	98	−17.7
	G79-K27	D80-R34	P55-K32	71	−17.4
	G79-K27	A57-R25	P55-K32	67	−17.7
	G79-R34	A57-R25	P55-K32	74	−18.6
	G79-R34	A57-R25	Y78-K27	63	−18.6
	G79-R34	D80-S37	A57-R25	49	−18.4
20	G79-K27	D80-R34	P55-S37	76	−16.2
	G79-K18	D80-E5	Y78-R19	43	−17.4
	G79-K18	Y78-R19	A54-K31	36	−17.7
	G79-K27	D80-R34	P55-K31	31	−16.7
21	G79-K27	P55-S37	D80-R34	106	−17.2
	G79-K27	P55-R25	G56-S37	39	−17.0
22	G79-K27	D80-R34	A57-K25	79	−15.2
	G79-K27	D80-R34	P55-S37	29	−15.0

F, number of successfully docked complexes out of 3000 attempts; G_{elec}, average electrostatic interaction free energy between the two proteins (kcal/mol).

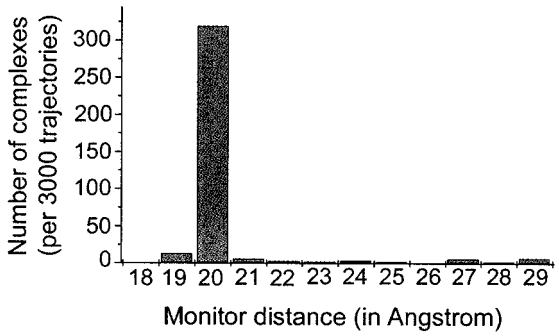

FIGURE 3 The distribution of distances between the two monitors for all complexes of the 16th structure of Lq2 associating with the K^+ channel. (The monitor distances shorter than 30 Å were recorded.)

two are not sufficient. During this process, we modified the criterion of the triplet contact of MacroDox. We initially analyzed the favorable triplet pairs between Lq2 and the K^+ channel using a triplet contact distance <5.5 Å. The distribution frequency and average electrostatic potential of the four favorable complexes derived from this cycle of analysis are listed in Table 2. It was noticed that Arg25 (Lq2) mainly interacts with Pro55, Gly56 and Asp80 of the K^+ channel, Lys27 (Lq2) with Tyr78 and Gly79, Lys31 (Lq2) with Pro55 and Gly56, and that Arg34 (Lq2) mainly interacts with Gly79 and Asp80 (Table 2). To get the more favor complexes, we performed a further analysis, focusing on triplet contact distances within 5.0 Å (Table 3). This tighter contact analysis resulted in the 16th structure of Lq2 having the highest frequency for matching the triplet contact criteria and the lowest electrostatic potential for binding with the K^+ channel (Table 3). This observation revealed that the 16th structure of Lq2, among the 22 available structures in the PDB file, is the most favorable binding conformation to the K^+ channel.

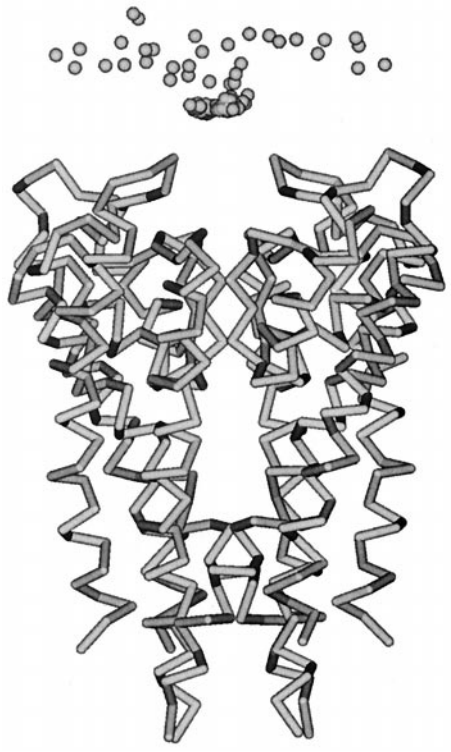

FIGURE 4 Distribution of the 16th structure of Lq2 around the extracellular entry mouth of the K^+ channel. The K^+ channel is represented as a C_α trace. Each dot represents the center of mass of Lq2 in an encounter snapshot with the K^+ channel.

TABLE 2 Possible triplet contacts for structures 5, 7, 15, and 16 of Lq2 interacting with the K^+ channel (contact distance less than 5.5 Å)

Structure	Triplets (K^+ channel res-Lq2 res)			F	G_{elec}
5	G79-K27	D80-R25	G56-K31	25	−22.8
	G79-K27	D80-R34	P55-K31	9	−21.3
	G79-K27	D80-R25	P55-K31	5	−20.7
	G79-K27	D80-R25	Y78-R34	0	
	G79-K27	D80-R25	P55-K32	0	
7	Y78-K27	G79-R34	G56-R25	55	−22.1
	G79-K27	D80-R34	G56-R25	14	−22.1
	Y78-K27	D80-R34	G56-R25	14	−22.1
	Y78-K27	G79-R34	A57-R25	3	−22.1
	G79-K27	D80-R34	A57-R25	0	
	Y78-K27	D80-R34	A57-R25	0	
15	Y78-K27	D80-R34	P55-K31	144	−23.7
	G79-K27	D80-R34	P55-K31	144	−23.7
16	G79-K27	D80-R34	P55-R25	194	−22.8
	Y78-K27	D80-R34	P55-R25	206	−22.8
	Y78-K27	G79-R34	P55-R25	247	−22.8

F, number of successfully docked complexes out of 3000 attempts; G_{elec}, average electrostatic interaction free energy between the two proteins (kcal/mol).

TABLE 3 Possible triplet contacts for structures 5, 7, 15, and 16 of Lq2 interacting with the K^+ channel (contact distance less than 5.0 Å)

Structure	Triplets (K^+ channel res-Lq2 res)			F	G_{elec}
5	G79-K27	D80-R25	G56-K31	0	
	G79-K27	D80-R34	P55-K31	4	−21.1
	G79-K27	D80-R25	P55-K31	0	
7	Y78-K27	G79-R34	G56-R25	36	−22.2
	G79-K27	D80-R34	G56-R25	0	
	Y78-K27	D80-R34	G56-R25	0	
	Y78-K27	G79-R34	A57-R25	0	
15	Y78-K27	D80-R34	P55-K31	1	−23.9
	G79-K27	D80-R34	P55-K31	1	−23.9
16	Y78-K27	G79-R34	P55-R25	129	−23.1
	Y78-K27	D80-R34	P55-R25	83	−23.1
	G79-K27	D80-R34	P55-R25	64	−22.8
	Y78-K27	G79-R34	P55-K31	47	−23.6

F, number of successfully docked complexes out of 3000 attempts; G_{elec}, average electrostatic interaction free energy between the two proteins (kcal/mol).

Contacts between Lq2 and K^+ channel

Employing BD simulations followed by a triplet contact analysis, we obtained a favorable association complex formed between Lq2 and the K^+ channel. The BD trajectories of the 16th structure of Lq2 gave 371 complex candidates with the K^+ channel. The distribution of Lq2 around the K^+ channel is presented in Fig. 4, which indicates that Lq2 is located in the extracellular entryway of the K^+ channel. This is in good agreement with the electrostatic potential calculations (Fig. 1).

We isolated the most stable structure having the strongest electrostatic interaction energy (−24.1 kcal/mol) and used it to analyze the contacts between Lq2 and the K^+ channel. The structure of this complex was subjected to energy minimization using the adopted-basis Newton Raphson algorithm and the CHARMm22 force field in Quanta. The optimized structure of the complex is shown in Fig. 5. In general, Lq2 binds to the K^+ channel mainly via its β-sheet, whereas its α-helix is far away from the interaction surface of the K^+ channel. This is in agreement with the mutagenesis experiments of Stampe et al. (1994), which showed that eight residues, namely, Ser10, Trp14, Arg25, Lys27, Met29, Asn30, Arg34, and Tyr36, are crucial for the binding function of CTX with the K^+ channel. Except for Ser10 and Trp14, all other residues are in the β-sheet of CTX. We do not see any interactions between Trp14 and the K^+ channel from our BD simulations. Mutagenesis experiments of Goldstein et al. (1994) seem to support the idea that Trp14 is a less critical residue than the others. The principal Lq2-K^+ channel interactions derived from the refined structure were analyzed and displayed using the LIGPLOT program (Wallace et al., 1995; McDonald and Thornton, 1994), which is shown in Fig. 6. The hydrogen bond and hydrophobic contact parameters are listed in Tables 4 and 5. Eleven hydrogen bonds are formed between Lq2 and K^+ channel, viz., residue Arg25 (Lq2) to one Pro55 (C) residue of K^+ channel, Lys27 (Lq2) to three Tyr78 (A-C) residues, Cys28 (Lq2) to Tyr82 (B), Arg31 (Lq2) to Pro55 (B), Arg34 (Lq2) to Gly79 (D) (two hydrogen-bonds), and Tyr36 (Lq2) to Tyr78 (C and D) (two hydrogen bonds) and Tyr82 (D). Thirteen hydrophobic contacts are formed between Lq2 and K^+ channel, viz., two hydrophobic contacts for Lys27 (Lq2) with Gly79 (B), two for Met29 (Lq2) with Tyr82 (A), one for Asn30 (Lq2) with Ala58 (A), one for Lys31 (Lq2) with Pro55 (B), and seven for Tyr36 (Lq2) with Gly79 (C), Asp80 (C), and Tyr82 (D) (Fig. 6).

According to the mutation experiments of Goldstein et al. (1994), 5 residues of CTX are critical for *Shaker* K^+ channel binding affinity: Lys27, Met29, Asn30, Arg34, and Tyr36. These residues conserved in CTX and Lq2 (Fig. 7) are found to be important in our study. From Tables 4 and 5, we can see that residues Lys27 and Arg34 of Lq2 form hydrogen bonds with the K^+ channel, Met29 and Asn30 bind with the K^+ channel through hydrophobic interactions, and Tyr36 interacts with the K^+ channel using both hydrogen bonding and hydrophobic interactions. Fig. 5 shows that the positively charged side chain of residue Lys27 (Lq2) apparently plugs the pore of K^+ channel and forms three hydrogen-bonds with the carbonyl groups of the backbones of Tyr78 residues of the K^+ channel. Both Lys27 (K27) and Tyr78 (Y78) are very conserved in the scorpion toxin and K^+ channel families, respectively (Miller, 1995; Hegin-

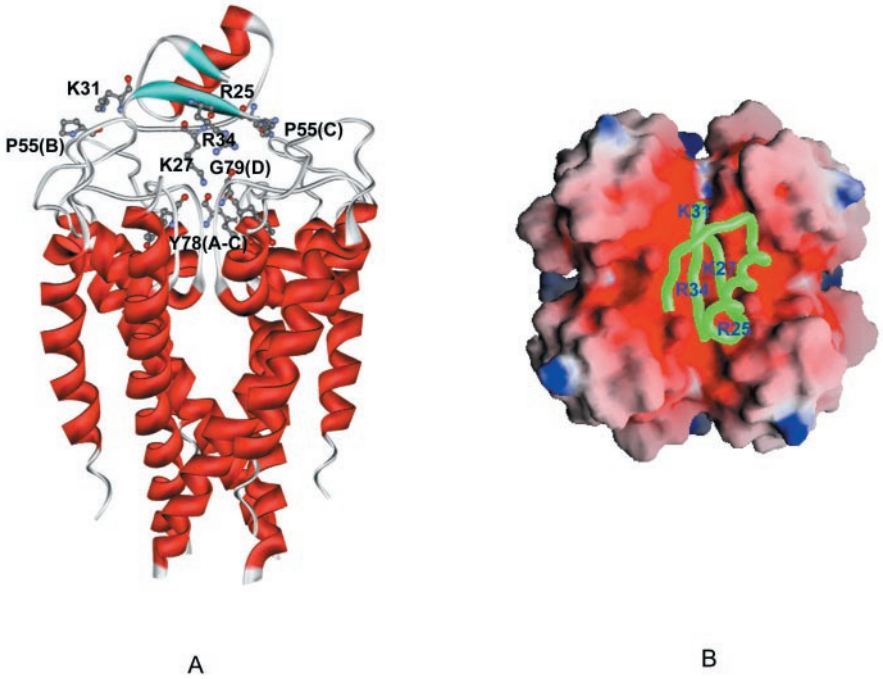

FIGURE 5 A typical final complex of the 16th structure of Lq2 and the K^+ channel. (*A*) The two molecules are represented as ribbon structures. The closest contacts Lys27-Tyr78 (A–C), Arg25-Pro55 (C), Lys31-Pro55 (B), and Arg34-Gly79 (D) are shown. (*B*) The top view of the complex shown in *A*, which was generated with the program GRASP (Nicholls et al., 1991). The K^+ channel represents as a molecular surface color coded by electrostatic potential and Lq2 as a green worm-like structure.

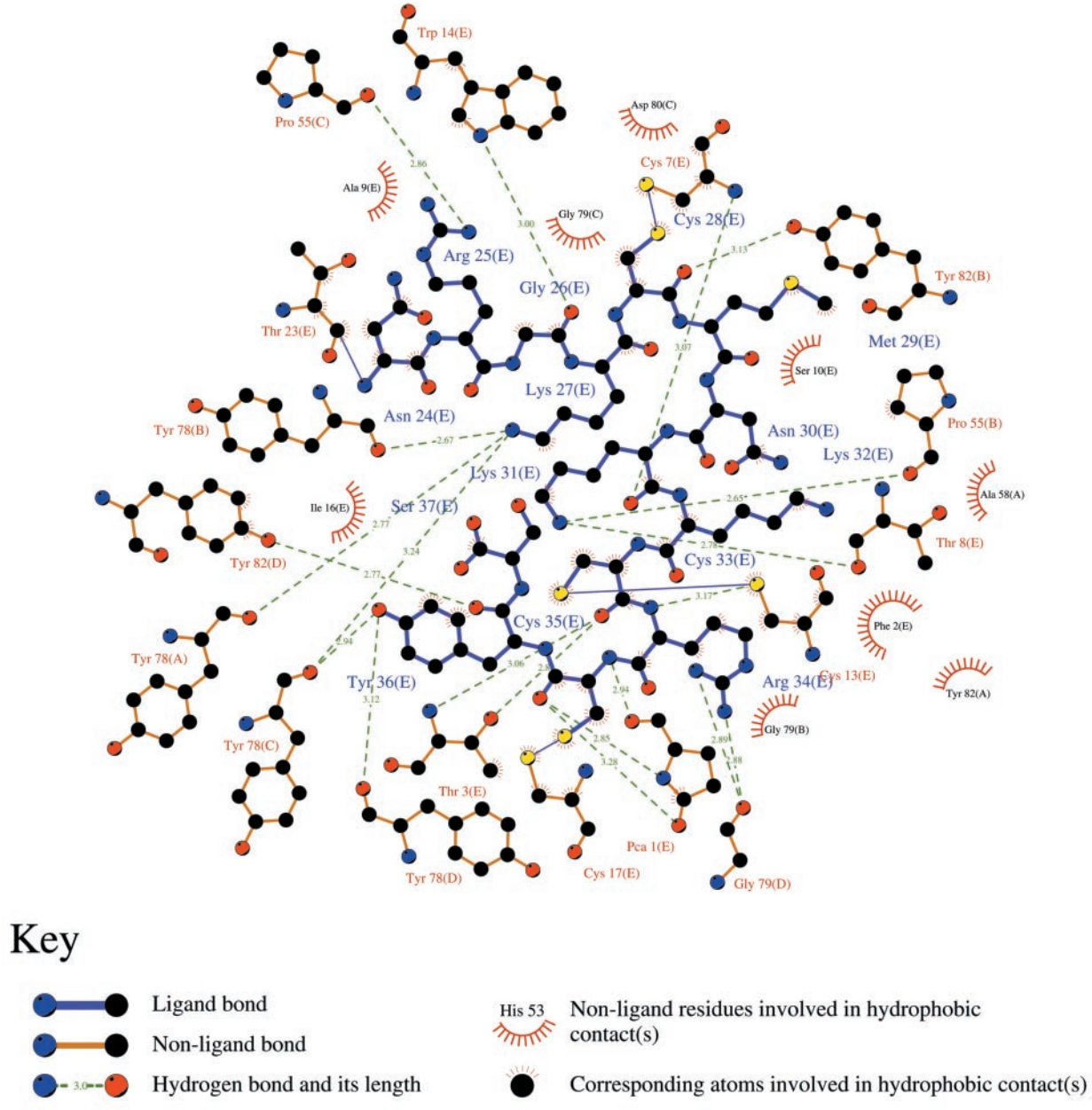

FIGURE 6 Schematic depiction (generated by LIGPLOT) of the main interactions between the Lq2 scorpion toxin and the K^+ channel.

botham et al., 1992, 1994). In the *Shaker* channel, the K27Q mutation results in a decrease in the binding affinity for the toxin significantly (15,000-fold; Goldstein et al., 1994). The 3D model of the Lq2-K^+ channel complex derived from the BD simulations, followed by molecular mechanics minimization, can explain the decrease in affinity due to this mutation. The importance of Lys27 was also highlighted by the mutation of K27R. The conservative mutation of this lysine of the CTX to arginine, with the same positive charge, destabilized the interaction with the toxin by over 1000-fold (Miller, 1995; Naranjo and Miller, 1996). Structurally, the side chain of arginine is longer than that of lysine, and the cationic terminus of arginine is larger. This renders the arginine side chain too close to the backbone carbonyls of Tyr78 in the pore of the K^+ channel, which decreases binding affinity with the K^+ channel. The R34Q mutation in CTX led to a 300-fold loss in binding affinity with the *Shaker* K^+ channel. From our study, Arg34 binds to the backbone carbonyl groups of Gly79 through two hydrogen bonds (Goldstein et al., 1994). Mutagenesis studies also indicated that residue Arg34 is critical for the binding of CTX to the Ca^{2+}- and voltage-activated K^+

TABLE 4 The hydrogen-bonds between the Lq2 scorpion toxin and the K^+ channel in the Lq2-K^+ channel complex

	Scorpion Toxin Lq2		K^+ channel	
Distance (Å)	Residue	Atom	Residue*	Atom
2.86	Arg25	NH1	Pro55(C)	O
2.67	Lys27	NZ	Try78(A)	O
2.77	Lys27	NZ	Try78(B)	O
3.24	Lys27	NZ	Try78(C)	O
3.13	Cys28	O	Tyr82(B)	OH
2.65	Lys31	NZ	Pro55(B)	O
2.89	Arg34	NH1	Gly79(D)	O
2.88	Arg34	NH2	Gly79(D)	O
2.77	Tyr36	O	Tyr82(D)	OH
2.94	Tyr36	OH	Tyr78(C)	O
3.12	Tyr36	OH	Tyr78(D)	O

The 3D model of the complex was constructed based on the BD simulations and molecular mechanics structural refinement for the 16th structure of Lq2 associating with the K^+ channel.
*A, B, C, and D represent the four chains of the K^+ channel.

channels (Park and Miller, 1992; Stampe et al., 1994; Goldstein et al., 1994; Naranjo and Miller, 1996). Naranjo and Miller (1996) found that the mutation M29I of CTX weakens block affinity by 1700-fold when tested on *Shaker* T449F. Our simulation results indicate that Met29 of Lq2 interacts with Y82 of the K^+ channel through two hydrophobic contacts, Tyr82 of KcsA is the counterpart to Thr449 in the *Shaker* K^+ channel (see Fig. 7). The N30Q and Y36Q mutations decrease the binding affinity of CTX with the *Shaker* K^+ channel by factors of 4900 and 7900, respectively (Goldstein et al., 1994). BD simulation and structural optimization found that Asn30 residue has one hydrophobic contact with Ala58, whereas Tyr36 has three hydrogen bonds and seven hydrophobic contacts with Tyr78, Gly79,

TABLE 5 The hydrophobic contacts between the Lq2 scorpion toxin and K^+ channel in the Lq2-K^+ channel complex

	Scorpion Toxin Lq2		K^+ channel	
Distance (Å)	Residue	Atom	Residue*	Atom
3.84	Lys27	CE	Gly79(B)	C
3.89	Lys27	CE	Gly79(B)	CA
3.56	Met29	CE	Tyr82(A)	CE1
3.89	Met29	CE	Tyr82(A)	CZ
3.67	Asn30	CG	Ala58(A)	CB
3.85	Lys31	CE	Pro55(B)	CB
3.49	Tyr36	CE2	Tyr82(D)	CE1
3.51	Tyr36	CD2	Tyr82(D)	CE1
3.54	Tyr36	CD2	Asp80(C)	CA
3.63	Tyr36	CD2	Tyr82(D)	CZ
3.67	Tyr36	CE2	Gly79(C)	C
3.75	Tyr36	CD2	Gly79(C)	C
3.75	Tyr36	CD2	Asp80(C)	CB

The 3D model of the complex was constructed based on the BD simulations and molecular mechanics structural refinement for the 16th structure of Lq2 associating with the K^+ channel.
*A, B, C and D represent the four chains of the K^+ channel.

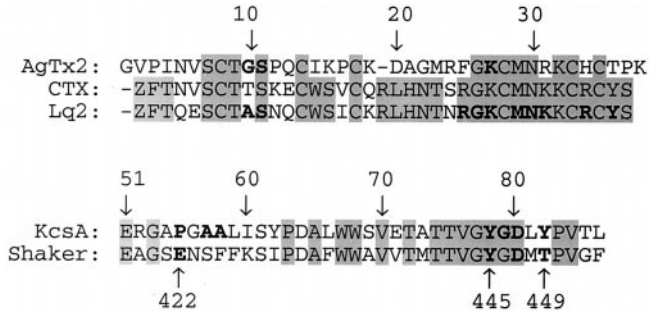

FIGURE 7 The sequences alignment of Lq2, CTX, AgTx2, KcsA (triple mutated), and *Shaker* K^+ channel. The conserved residues are highlighted, and the residues that form contacts with KcsA are bloated and highlighted.

Asp80, and Tyr82 of the K^+ channel (Table 5 and Fig. 6). Other important residues of Lq2 that interact with the K^+ channel are Arg25 and Lys31. The side chain of Arg25 binds to the backbone carbonyl group of Gly56, whereas Lys31 hydrogen bonds to the backbone carbonyl groups of Pro55 and interacts with this residue with a hydrophobic contact. Charge mutations introduced at residue Glu422 of the *Shaker* K^+ channel, which is the counterpart of residue Pro55 of KcsA (see Fig. 7), were found to affect toxin affinity. The charge-altering mutations introduced at position 422 in the *Shaker* K^+ channel from negative to positive lowered the association rate constant (Escobar et al., 1993), indicating that residue 422 of the *Shaker* channel is close to the positive electrostatic potential of the toxin. Our BD simulations and molecular mechanics structural refinement showed that this potential is mainly formed by the side chains of Arg25 and Lys31. These data are consistent with the BD simulation results.

Another closely related homologue toxin of Lq2 is AgTx2 (Park and Miller, 1992). The change in binding free energy caused by single residue mutations on AgTx2 showed that the energetically important residues of AgTx2 fall into three regions: the residues at the beginning of an α-helix (Gly10 and Ser11), the residues along with the second β-strand (Arg24-Asn30), and the residues at the end of the third β-strand (Thr36 and Pro37; Ranganathan et al., 1996). BD simulation indicated that the Lq2 binds with the K^+ channel in a similar way of AgTx2, also using three main regions: Ala9 and Ser10 at the beginning of the α-helix, Arg25 and Lys27-Lys31 of the second β-strand, and Arg34 and Tyr36 of the third β-strand. In addition, thermodynamic mutant cycle analysis also suggested that the residues Gly10 and Ser11 of AgTx2 may interact with Phe425 and Asp447 of the *Shaker* K^+ channel, and Lys27 of AgTx2 may couple with Tyr445 of *Shake* K^+ channel (Ranganathan et al., 1996). This is also in general agreement with the BD simulation results. The sequence alignment of AgTx2, CTX and Lq2 is shown in Fig. 7. The sequence identity between Lq2 and CTX is ~78.4%, and that between Lq2 and AgTx2 is ~43.2%. The 3D structure ho-

mology between these three toxins is much higher: structural alignment showed that the RMSD of C_α atoms between Lq2 and CTX is ~1.62 Å, and that between Lq2 and AgTx2 is ~1.68 Å. This indicates that, like CTX, AgTx2 should bind with K^+ channel in a similar way. This further demonstrates the reasonability and reliability of our BD simulation results.

CONCLUSION

We have obtained a good 3D model of the Lq2-K^+ channel complex through Brownian dynamics simulations and molecular mechanics structural refinement (Fig. 5). BD simulations predict that the β-sheet of Lq2 associates with the extracellular entryway of the K^+ channel, which is in line with the primary clues from the electrostatic potential calculations (Fig. 1) and mutagenesis results (Stampe et al., 1994). Our docking process overcame some of the disadvantages of BD, i.e., it cannot easily consider the conformational flexibility of the associating proteins. We noticed that the conformation indeed affected the simulation results; only four structures among the 22 available NMR structures of Lq2 located themselves around the binding site of the K^+ channel with high frequencies. Triplet contact analyses using modified criteria, along with electrostatic interaction free energies calculations, further demonstrated that the 16th structure in 1LIR is the best conformation for the scorpion toxin Lq2 to bind with the K^+ channel. It is remarkable that our 3D model of the Lq2-K^+ channel complex constructed with the results of BD simulations followed by molecular mechanics structural refinement, can be used to explain most of the experimental phenomena for the binding of scorpion toxins (such as CTX and AgTx2), either in their wild-type or mutants, to the K^+ channel. The consistency between the results of the BD simulations and the experimental data indicated that our 3D model of the Lq2-K^+ channel complex is reasonable and can be used in further biological studies, such as rational design of the blocking agents of K^+ channels and mutagenesis in both toxin and K^+ channels.

We thank Professor S. H. Northrup for his kindness in offering us the MacroDox 3.2.2 program and his helpful discussions. We gratefully acknowledge financial support from the National Natural Science Foundation of China (grant 29725203) and the State Key Program of Basic Research of China (grant 1998051115). The calculations were performed on Origin 2000 at the Network Information Center, Chinese Academy of Science, Shanghai Branch.

REFERENCES

Bernstein, F. C., T. F. Koetzle, G. J. Williams, E. E. Meyer, Jr., M. D. Brice, J. R. Rodgers, O. Kennard, T. Shimanouchi, and M. Tasumi. 1977. The Protein Data Bank: a computer-based archival file for macromolecular structures. *J. Mol. Biol.* 112:535–542.

Catterall, W. A. 1988. Structure and function of voltage-sensitive ion channels. *Science.* 242:50–61.

Doyle, D. A., J. Morais Cabral, R. A. Pfuetzner, A. Kuo, J. M. Gulbis, S. L. Cohen, B. T. Chait, and R. MacKinnon. 1998. The structure of the potassium channel: molecular basis of K+ conduction and selectivity. *Science.* 280:69–77.

Ermak, D. L., and J. A. McCammon. 1978. Brownian dynamics with hyrodynamic interactions. *J. Chem. Phys.* 69:1352–1360.

Escobar, L., M. J. Root, and R. MacKinnon. 1993. Influence of protein surface charge on the bimolecular kinetics of a potassium channel peptide inhibitor. *Biochemistry.* 32:6982–6987.

Gabdoulline, R. R., and R. C. Wade. 1998. Brownian dynamics simulation of protein-protein diffusional encounter. *Methods: Meths. Enzymol.* 14: 329–341.

Goldstein, S. A., D. J. Pheasant, and C. Miller. 1994. The charybdotoxin receptor of a Shaker K+ channel: peptide and channel residues mediating molecular recognition. *Neuron.* 12:1377–1388.

Heginbotham, L., T. Abramson, and R. MacKinnon. 1992. A functional connection between the pores of distantly related ion channels as revealed by mutant K+ channels. *Science.* 258:1152–1155.

Heginbotham, L., Z. Lu, T. Abramson, and R. MacKinnon. 1994. Mutations in the K+ channel signature sequence. *Biophys. J.* 66:1061–1067.

Kaczorowski, G. J., and M. L. Garcia. 1999. Pharmacology of voltage-gated and calcium-activated potassium channels. *Curr. Opin. Chem. Biol.* 3:448–458.

Lu, Z., and R. MacKinnon. 1997. Purification, characterization, and synthesis of an inward-rectifier K+ channel inhibitor from scorpion venom. *Biochemistry.* 36:6936–6940.

Lucchesi, K., A. Ravindran, H. Young, and E. Moczydlowski. 1989. Analysis of the blocking activity of charybdotoxin homologs and iodinated derivatives against Ca2+-activated K+ channels. *J. Membr. Biol.* 109:269–281.

MacKinnon, R., S. L. Cohen, A. Kuo, A. Lee, and B. T. Chait. 1998. Structural conservation in prokaryotic and eukaryotic potassium channels. *Science.* 280:106–109.

MacKinnon, R., L. Heginbotham, and T. Abramson. 1990. Mapping the receptor site for charybdotoxin, a pore-blocking potassium channel inhibitor. *Neuron.* 5:767–771.

MacKinnon, R., and C. Miller. 1989. Mutant potassium channels with altered binding of charybdotoxin, a pore- blocking peptide inhibitor. *Science.* 245:1382–1385.

Madura, J. D., J. M. Briggs, R. C. Wade, M. E. Davis, B. A. Luty, A. Ilin, J. Antosiewicz, M. K. Gilson, B. Bagheri, L. R. Scott, and J. A. McCammon. 1995. Electrostatic and diffusion of molecules in solution: simulations with the University of Houston Brownian Dynamics Program. *Comp. Phys. Comm.* 91:57–95.

Matthew, J. B. 1985. Electrostatic effects in proteins. *Annu. Rev. Biophys. Biophys. Chem.* 14:387–417.

Matthew, J. B., and F. R. Gurd. 1986. Calculation of electrostatic interactions in proteins. *Methods Enzymol.* 130:413–436.

McDonald, I. K., and J. M. Thornton. 1994. Satisfying hydrogen bonding potential in proteins. *J. Mol. Biol.* 238:777–793.

Miller, C. 1995. The charybdotoxin family of K+ channel-blocking peptides. *Neuron.* 15:5–10.

Mintz, I. M., M. E. Adams, and B. P. Bean. 1992. P-type calcium channels in rat central and peripheral neurons. *Neuron.* 9:85–95.

Naranjo, D., and C. Miller. 1996. A strongly interacting pair of residues on the contact surface of charybdotoxin and a Shaker K+ channel. *Neuron.* 16:123–130.

Nicholls, A., K. A. Sharp, and B. Honig. 1991. Protein folding and association: insights from the interfacial and thermodynamic properties of hydrocarbons. *Proteins.* 11:281–296.

Northrup, S. H., J. O. Boles, and J. C. L. Reynolds. 1987. Electrostatic Effects in the Brownian dynamics of Association and Orientation of heme Protein. *J. Phys. Chem.* 91:5991–5998.

Northrup, S. H., T. Laughner, and G. Stevenson. 1999. MacroDox Macromolecular Simulation Program. Tennessee Technological University, Department of Chemistry, Cookeville, TN.

Northrup, S. H., K. A. Thomasson, C. M. Miller, P. D. Barker, L. D. Eltis, J. G. Guillemette, S. C. Inglis, and A. G. Mauk. 1993. Effects of charged amino acid mutations on the bimolecular kinetics of reduction of yeast iso-1-ferricytochrome c by bovine ferrocytochrome b5. *Biochemistry.* 32:6613–6623.

Ouporov, IV, H. R. Knull, and K. A. Thomasson. 1999. Brownian dynamics simulations of interactions between aldolase and G- or F-actin. *Biophys. J.* 76:17–27.

Park, C. S., and C. Miller. 1992. Mapping function to structure in a channel-blocking peptide: electrostatic mutants of charybdotoxin. *Biochemistry.* 31:7749–7755.

Pearson, D. C., Jr., and E. L. Gross. 1998. Brownian dynamics study of the interaction between plastocyanin and cytochrome f. *Biophys. J.* 75: 2698–2711.

Ranganathan, R., J. H. Lewis, and R. MacKinnon. 1996. Spatial localization of the K+ channel selectivity filter by mutant cycle-based structure analysis. *Neuron.* 16:131–139.

Renisio, J. G., Z. Lu, E. Blanc, W. Jin, J. H. Lewis, O. Bornet, and H. Darbon. 1999. Solution structure of potassium channel-inhibiting scorpion toxin Lq2. *Proteins.* 34:417–426.

Smoluchowski, M. V. 1917. Versuch einer mathematischen Theorie der Koagulationskinetik Kolloider Loeschungen. *Z. Phys. Chem.* 92: 129–168.

Stampe, P., L. Kolmakova-Partensky, and C. Miller. 1994. Intimations of K+ channel structure from a complete functional map of the molecular surface of charybdotoxin. *Biochemistry.* 33:443–450.

Wallace, A. C., R. A. Laskowski, and J. M. Thornton. 1995. LIGPLOT: a program to generate schematic diagrams of protein-ligand interactions. *Protein Eng.* 8:127–134.

Warwicker, J., and H. C. Watson. 1982. Calculation of the electric potential in the active site cleft due to alpha-helix dipoles. *J. Mol. Biol.* 157: 671–679.